



Effect of sodium octanoate on the tribocorrosion behaviour of 5052 aluminium alloy

Hongjin Zhao, Lei Cao, Yong Wan & Jibin Pu

To cite this article: Hongjin Zhao, Lei Cao, Yong Wan & Jibin Pu (2018) Effect of sodium octanoate on the tribocorrosion behaviour of 5052 aluminium alloy, Tribology - Materials, Surfaces & Interfaces, 12:4, 200-207, DOI: [10.1080/17515831.2018.1531651](https://doi.org/10.1080/17515831.2018.1531651)

To link to this article: <https://doi.org/10.1080/17515831.2018.1531651>



Published online: 11 Oct 2018.



Submit your article to this journal [↗](#)



Article views: 7



View Crossmark data [↗](#)



Effect of sodium octanoate on the tribocorrosion behaviour of 5052 aluminium alloy

Hongjin Zhao^a, Lei Cao^a, Yong Wan^a and Jibin Pu^b

^aSchool of Mechanical & Automotive Engineering, Qingdao University of Technology, Qingdao, People's Republic of China; ^bKey Laboratory of Marine New Materials and Related Technology, Zhejiang Key Laboratory of Marine Materials and Protection Technology, Ningbo Institute of Material Technology and Engineering, Chinese Academy of Sciences, Ningbo, People's Republic of China

ABSTRACT

The 5000 series aluminium alloys are commonly used in a marine application where it is exposed to environments containing the chloride ions, which cause corrosion of aluminium alloy. The situation becomes even worse when aluminium alloys, in some situations, may suffer from combined corrosion and wear actions. The present study has been carried out to investigate the effect of sodium octanoate as a corrosion inhibitor on the corrosive wear behaviour of aluminium alloy 5052 in 0.5 M NaCl solution as simulated seawater. The effects of electrochemical potentials on the corrosive wear performance are also discussed.

ARTICLE HISTORY

Received 14 March 2018
Accepted 26 September 2018

KEYWORDS

Aluminium alloy; sodium octanoate; tribocorrosion; sodium chloride

1. Introduction

The aluminium alloys are commonly used in various industrial areas due to their excellent mechanical properties, low density, good conductivity, thermal conductivity and corrosion resistance [1,2]. Their corrosion-inhibiting performance is from a compact, strongly adherent and protective surface oxide film which is developed on aluminium alloys upon exposure to the atmosphere or aqueous solutions. However, in a marine application, the presence of chloride ions in the solution causes pitting corrosion of aluminium alloy [3,4]. The situation becomes ever worse when aluminium alloy, in some situations, may suffer from combined corrosion and wear actions, i.e. tribocorrosion process [5,6]. During the tribocorrosion process, accelerated wear was always observed for various metal materials by combining mechanical, chemical and electrochemical factors [7–15].

Some inorganic and organic inhibitors, such as rare-earth compounds [16,17], 1,4-naphthoquinone [18], sodium decanoate [19] are added as the corrosion-inhibitors to reduce the corrosion of aluminium. Among them, salt of monocarboxylic acids is environmentally friendly and known to prevent corrosion for various metals [19–22]. However, there are few papers available which deal with the effects of alkyl carboxylates on tribocorrosion behaviour of aluminium in corrosive media containing Cl^- ions. In this work, the effect of sodium octanoate on tribocorrosion behaviour of 5052 aluminium alloy (AA5052) sliding against an alumina ball in 0.5 M NaCl solution have been investigated by measuring the coefficients of friction, the

electrochemical response and total metal losses. The experiments have been conducted under potentiostatic conditions at a wide range of potentials to study the effect of applied electrochemical potentials on frictional and wear behaviour of AA5052. The overall tribocorrosion behaviour is discussed.

2. Experimental

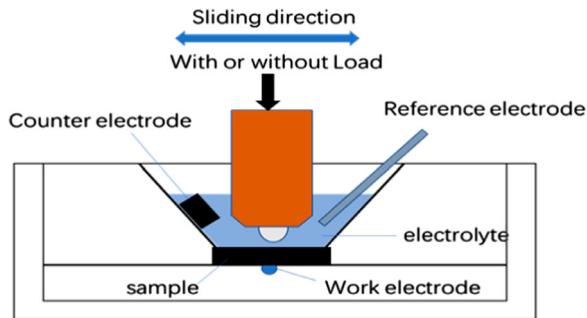
Sodium chloride (99.5% in purity, NaCl) and sodium octanoate (>99% in purity, $\text{C}_7\text{H}_{15}\text{COO}^- \text{Na}^+$, denoted as C8Na hereafter) were obtained commercially and used without further purification. All the test solutions were freshly prepared using distilled water. 0.5 M NaCl solution with varied concentration of C8Na (0.0025, 0.005, 0.01 and 0.02 M) were used as the testing solution.

The material used here is AA5052 with the major chemical compositions as shown in Table 1. The material was cut into specimen sizes of $36 \times 36 \times 1 \text{ mm}^3$. Before tribocorrosion testing, each specimen was wet ground using a series of SiC grinding papers down to grit 1500 emery paper, followed by cleaning in running water and then methanol.

The tribocorrosion tests were carried out using a ball-on-disk tribometer with connected with a potentiostat, manufactured by Lanzhou Huahui Instrumental Company. As shown in Figure 1, the ball was running against a stationary AA 5052 specimen held in the test cell in a reciprocated mode. The ball used in this work was an alumina ball of 6 mm in diameter. The test cell was filled with about 20 ml of the testing

Table 1. The major chemical compositions for AA5052.

Elements	Si	Cu	Mg	Zn	Mn	Cr	Fe	Al
Chemical compositions (wt%)	0.25	0.1	2.2–2.8	0.1	0.15–0.35	0.15–0.35	0.4	Balance

**Figure 1.** The scheme of the corrosion and tribocorrosion instrument.

solution. A three-electrode cell set-up was used that consists of an AA 5052 disk as working electrode (4.8 cm^2 exposed area), a graphite electrode as the auxiliary electrode, and a saturated Ag/AgCl electrode as the reference electrode. All the tests were performed at room temperature (25°C) and open to the air.

At first, the polarization curves were obtained potentiodynamically between potential ranges from -1.65 to -0.15 V with scan rates of 1 mV/s under both static immersion and abrasion conditions. Under static immersion condition, the experiments are conducted without applying the load, whereas under abrasion condition, alumina ball is sliding against AA5052 disk with the reciprocating stroke length of 6 mm and the sliding frequency of 1 Hz . The normal force was 2 N , which corresponds to an initial maximum Hertzian contact pressure of 0.52 GPa , calculated based on the contact between the alumina ball and the AA5052 flat surface. All the tests were carried out in de-aerated solutions under stirred conditions. The temperature was maintained at 25°C during the experiments by immersing the glass vessel in a thermostatically controlled water bath. Two potentiodynamic experiments for each sample have been conducted, but only one representative curve for each sample is illustrated because of to the similarity of the curves. The measured current-voltage data were plotted as Tafel plot in the form of potential versus $\log(i)$ (the current density). The corrosion potential (E_{corr}) and corrosion current (I_{corr}) were derived from the Tafel plot. The inhibition efficiency ($\%IE$) was calculated using the following equation:

$$\%IE = 1 - I_{\text{corr}}(i)/I_{\text{corr}}(o) \times 100$$

where $I_{\text{corr}}(i)$ is the corrosion current density with 0.5 M NaCl solution in presence of C8Na, $I_{\text{corr}}(o)$ is the corrosion current density 0.5 M NaCl solution in absence of C8Na.

Potentiostatic experiments were then conducted to determine the efforts of applied electrochemical potentials on frictional and wear behaviour of AA5052. The testing condition are as following: the reciprocating stroke length of 6 mm , the sliding frequency 1 Hz and the normal force was 2 N . The constant potential was applied for a total abrasion duration of 35 min in which 5 min before rubbing started, 25 min during rubbing and 5 min after the termination of rubbing. During whole duration of each test, the COF were recorded simultaneously. The tribocorrosion experiments were repeated three times for the same surface condition in order to validate the results obtained. After test, surface profile across the wear track was measured and used to estimate cross-sectional area of the wear track using a stylus profilometer (Form Taly-surf PGI 800, UK). The total wear volume was obtained by multiplying the cross-sectional area by the length of the wear track. The surface morphology of the tested specimens was examined by scanning electron microscopy (SEM). Because no measurable wear was found on the alumina ball for all the tests conducted, thus we did not discuss the tribocorrosion behaviour of the inert alumina ball in this paper.

3. Results

3.1. Potentiodynamic polarization behaviour

The experiments are firstly conducted to investigate the potentiodynamic behaviour of AA5052 samples under static immersion condition for NaCl solution in the absence and the presence of C8Na with different concentrations from 0.0025 to 0.02 M . The results are presented in Figure 2(a). The corresponding electrochemical parameters derived from polarization curves are summarized in Table 2. In the blank NaCl solution, the specimen suffers from general corrosion and then passivation when potentials are set from corrosion potential (-1.2 V vs Ag/AgCl) to -0.6 V vs Ag/AgCl. The pitting corrosion occurs above -0.6 V vs Ag/AgCl, as indicated by the rapid increase in current density. The addition of C8Na to NaCl solution leads to increase of corrosion and pitting potential. The corrosion-inhibiting effects are more evident at higher concentration of C8Na until a critical concentration of 0.01 M . An opposite behaviour was displayed when 0.02 M C8Na are added to NaCl solution. In this case, a rise in current density and a decrease in corrosion potential were observed. The tendency can be clearly observed in the change of inhibition efficiency with C8Na concentration, as shown in Figure 3.

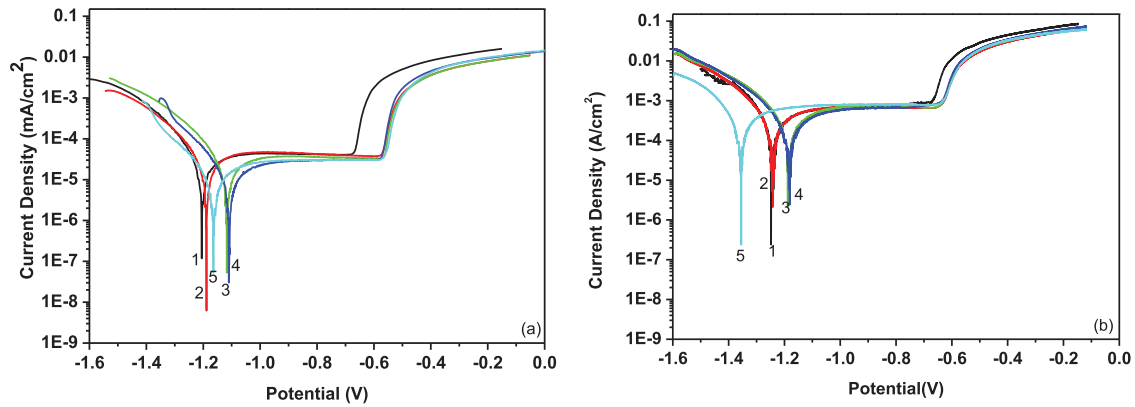


Figure 2. Potentiodynamic polarization curves recorded under (a) static immersion and (b) abrasion conditions in NaCl solution containing (1) 0 M, (2) 0.0025 M, (3) 0.005 M, (4) 0.01 M and (5) 0.02 M sodium octanoate.

Table 2. Electrochemical parameters for AA5052 determined from polarization curves under static immersion and abrasion conditions in NaCl solution containing sodium octanoate with various concentrations.

Concentration (M)	Static immersion			Abrasion		
	E_{corr} (V)	I_{corr} (mA/cm ²)	% IE	E_{corr} (V)	I_{corr} (mA/cm ²)	% IE
0	-1.20	45.0		-1.24	240	
0.0025	-1.19	23.8	47	-1.23	206	14
0.005	-1.11	18.9	58	-1.20	174	27
0.01	-1.10	7.7	83	-1.19	147	39
0.02	-1.17	15.0	67	-1.35	220	8

The effect of rubbing on the potentiodynamic behaviour of the AA5052 samples in NaCl solution in the absence and the presence of C8Na was then investigated by recording the polarization curves during sliding at a load of 2 N. The results are shown in Figure 2(b) and corresponding electrochemical parameters are summarized in Table 2. It is clearly observed that the corrosion potential is shifted cathodically under abrasion condition as comparing to static immersion condition in all cases. The current density is measured as 10 times larger under abrasion condition than under static immersion. However, C8Na is still effective in inhibiting the corrosion of AA5052 under abrasion condition. When C8Na is added to NaCl solution, both anodic and especially cathodic curves show lower current densities than those recorded in its absence. Corrosion potential values in the presence of C8Na are shifted in the positive direction. The corrosion-inhibiting effects are more evident at higher concentrations until a critical concentration of 0.01 M C8Na. Then a rise in the current density and decrease of corrosion potential was observed when 0.02 M C8Na is added. The similar situation is also indicated by the observing the convolution of inhibition efficiency with the concentration of C8Na in NaCl solution, as shown in Figure 3.

The tribological behaviour of aluminium was also evaluated during potentiodynamic test under abrasion condition. Figure 4 shows a variation of coefficient of friction (COF) as a function of sliding time and/or

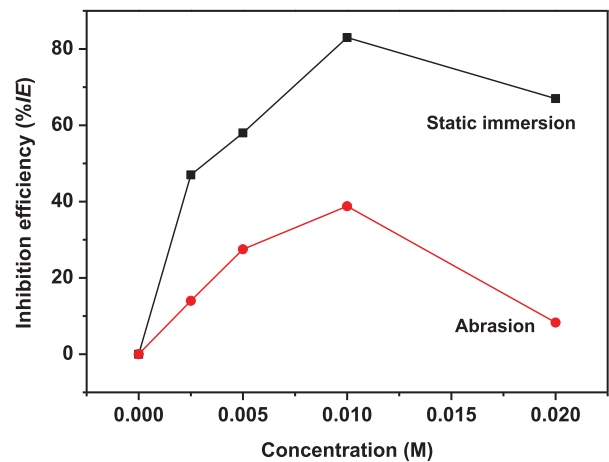


Figure 3. Change of inhibition efficiency of AA5052 in 0.5M NaCl solution containing C8Na with different concentrations under static immersion and abrasion conditions.

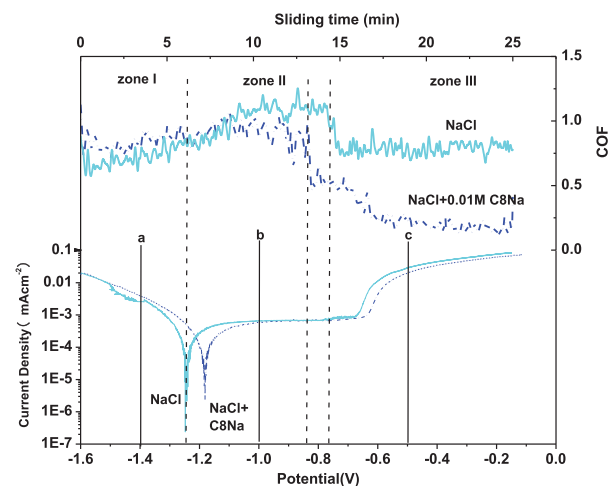


Figure 4. Polarization curve and coefficient of friction (COF) during the sliding test for the NaCl solution in the absence and presence of 0.01 M C8Na under abrasion condition. The vertical solid lines indicate the constant potentials at which sliding wear tests were conducted during following testing.

applied electrochemical potential for NaCl solution in the absence and the presence of 0.01 M C8Na. The polarization curve is also included. It is clearly observed

that the addition of C8Na is effective in reducing the friction, especially at higher potentials. Moreover, there exists the correlation between COF and current density arising from polarization. In general, three zones can be clearly observed in the friction curve. With the onset of potential sweep starting at a cathodic potential (-1.6 V vs Ag/AgCl), the COF experiences a small and slow rise to 1.1 until corrosion potential is set (zone I). In the zone II, the COF continues increasing slowly in the anodic region potential from the corrosion potential until certain potential (-0.73 V for NaCl solution or -0.84 V vs Ag/AgCl in presence of 0.01 M C8Na). Then a sudden decrease in COF were observed and the value of COF keep stable at 0.77 for NaCl solution. However, much lower stable COF of ~ 0.19 is found for NaCl solution containing 0.01 M C8Na.

Figure 5 shows the effect of the C8Na concentration on the COF and wear performance of AA5052 in the potentiodynamic test under abrasion condition. It is clearly observed that the addition of 0.0025 M C8Na is helpful in reducing the COF. No change in friction curve is observed when the concentration of C8Na is over 0.005 M. Though there is minor effort of C8Na

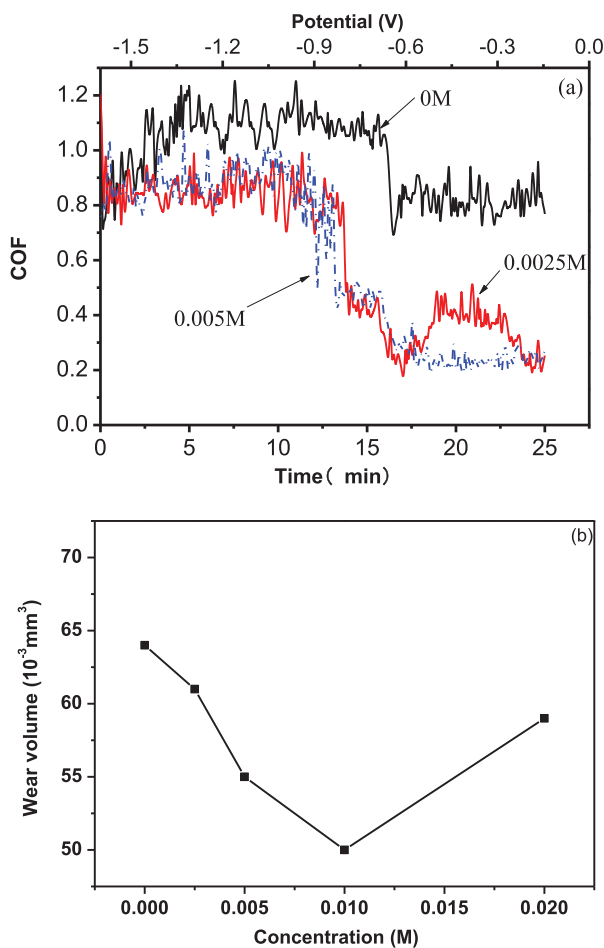


Figure 5. (a) The coefficient of friction (COF) during, and (b) wear volume after potentiodynamic test under abrasion condition for NaCl solution in the absence and presence of C8Na with different concentration.

concentration on COF, however, lower wear volumes are clearly observed for NaCl in presence of C8Na with its concentration until 0.01 M, and further increasing C8Na concentration produces larger wear. It is interesting to observe that the tendency to wear protection by C8Na parallels its corrosion-resistant performance, as shown in Figure 3.

3.2. Effect of applied potential on friction and wear

The different tribological performance of addition of C8Na to NaCl solution during potentiodynamic measure inspired us to investigate the effect of applied electrochemical potential on tribological performance of AA5052. In the next potentiostatic experiments, the constant potential was applied under a load of 2 N for a total duration of 35 min in which 5 min before rubbing started, 25 min during rubbing and 5 min after the termination of rubbing. During the whole duration of each test, the COF were recorded simultaneously. Relative to OCP, three potentials in both cathodic and anodic domains were selected. They are indicated by the arrowed vertical lines marked 'a' to 'c' in Figure 4 for polarization curves of AA5052. Specifically, -1.4 V vs Ag/AgCl was applied to shift the potential cathodically versus OCP, in order to suppress corrosion and provide the information of pure mechanical wear. -1.0 V vs Ag/AgCl was chosen to shift the potential anodically. The -0.5 V vs Ag/AgCl was selected in order to investigate the effort of pits formation on the tribological performance of AA5052.

The first experiment was conducted at a cathodic potential of -1.4 V vs Ag/AgCl (vertical line 'a' in Figure 4) in NaCl solution in the absence and the presence of 0.01 M C8Na. The evolution of current and COF with sliding time are recorded and shown in Figure 6. As expected, the current is cathodic in both testing solutions during the whole sliding duration.

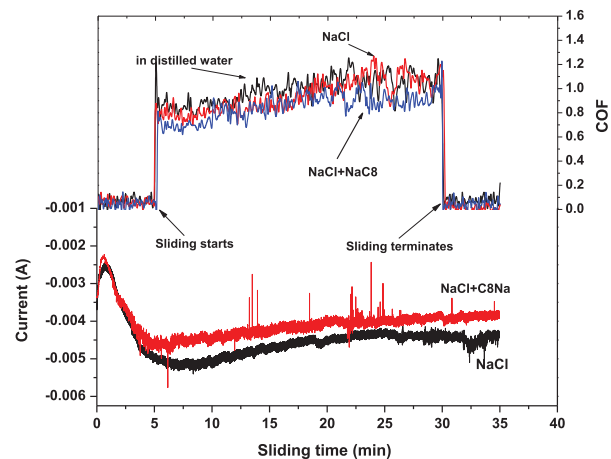


Figure 6. The convolution of current transient and coefficient of friction as function of sliding time before, during and after sliding test at a cathodic potential of -1.4 V vs Ag/AgCl.

The addition of C8Na to NaCl solution shows a tiny effect in increasing the current. Moreover, both solution show similar friction curve, in which the COF increases from 0.8 to 1.1 during the whole sliding process. Correspondingly, similar total wear volume is observed for NaCl solution in the absence and the presence of 0.01 M C8Na (see Figure 9(b) in the Discussion section).

Figure 7(a) shows the variation of current and COF with sliding time at anodic potentials of -1.0 V vs Ag/AgCl (vertical lines 'b' in Figure 4). When the blank NaCl solution is used, the current is measured to be anodic, which remains a stable value of about 7×10^{-4} A with sliding time until the end of sliding. The COF experiences a slow increase from around 0.8 to 1.1 during the whole sliding process. Addition of 0.01 M C8Na to NaCl solution clearly changes the electrochemical and frictional behaviour. The current increases to a value of 7×10^{-4} A once sliding and fluctuates for ~ 3 mins sliding. Then the current sharply decreases afterwards and keeps stable at a lower value of 6×10^{-4} A until end of sliding. The COF is stable at a lower value of 0.1 during the whole sliding. Correspondingly, much smaller wear volume is observed for NaCl solution in presence of 0.01 M C8Na than its absence (see Figure 9(b) in the Discussion section). SEM observation (Figure 7(b)) shows that the wear

track in the blank NaCl solution is populated with an accumulation of wear debris inside and on the edge of wear track. On the other hand, the wear track (Figure 7(c)) for NaCl solution with C8Na is smooth.

At -0.5 V vs Ag/AgCl (vertical line 'c' in Figure 4), which is above the pitting potential under both static immersion and abrasion condition, the measured current is increased by two orders of magnitude than that at -1.0 V (Figure 8(a)) in both testing NaCl solutions. The more striking effect can be observed for the blank NaCl solution than NaCl solution containing 0.01 M C8Na. Similar friction curves are found for both solutions. Figure 8(b) is for SEM image of wear track from the blank NaCl solution, showing several large pits in the wear track. However, less pits are observed inside the wear track from the NaCl solution containing 0.01 M C8Na (Figure 8(c)). Only the peel-off of surface film is observed. This is also indicated in the measured total wear volume, in which smaller wear is observed when C8Na is added to NaCl solution (see Figure 9(b) in the Discussion section).

4. Discussion

The results from potentiodynamic polarization experiments clearly show that C8Na molecules are effective in inhibiting the corrosion of aluminium in 0.5 M

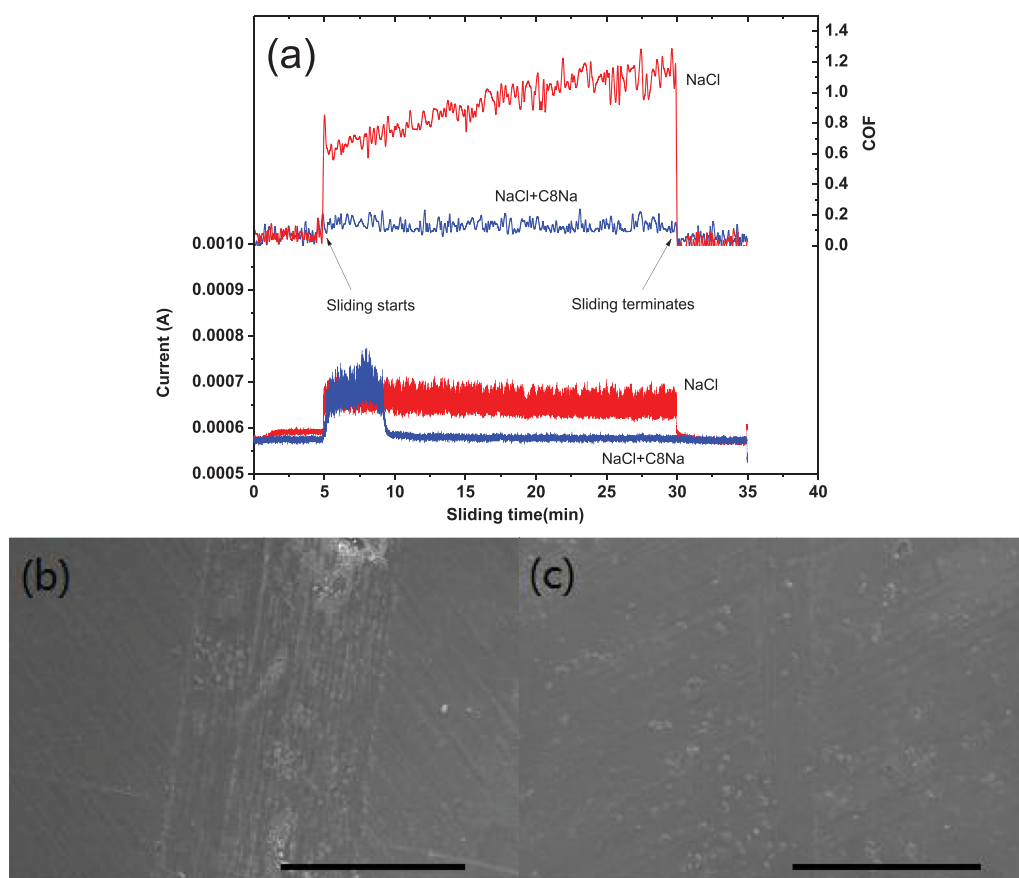


Figure 7. (a) The convolution of current transient and coefficient of friction as function of sliding time before, during and after sliding test at an anodic potential -1.0 V vs Ag/AgCl. SEM image of the wear track produced at -1.0 V vs Ag/AgCl for (b) NaCl solution and (c) NaCl solution containing 0.01 M C8Na. Scale bar: 100 μ m.

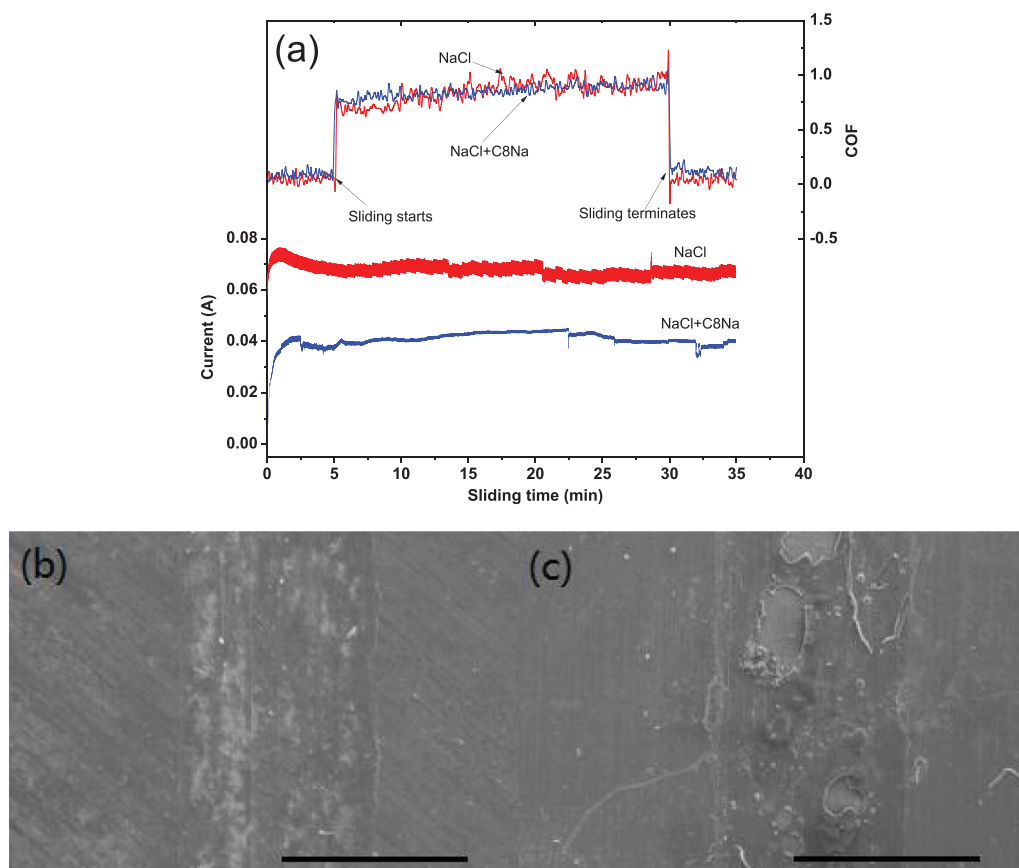


Figure 8. (a) The convolution of current transient and coefficient of friction as function of sliding time before, during and after sliding test at -0.5 V vs Ag/AgCl. SEM image of the wear track produced at an anodic potential -0.5 V for NaCl solution in (b) the absence and (c) presence of 0.01 M sodium octanoate. Scale bar: 100 μm .

NaCl solution under both static immersion and abrasion conditions. The C8Na is an anionic surfactant with the carboxylate polar head and long alkyl hydrophobic tail. The corrosion-inhibition mechanism of aluminium by octanoate anion is described before as the hydrophobic character of the aluminium carboxylate film which is obtained by adsorption of octanoate anion onto the aluminium surface [19]. The inhibitive organic film is water repellent and forms a barrier for mass and charge transfer, which leads to a protection of the metal surface from the attack of chloride ions. Thus, C8Na is acting as an adsorption-type inhibitor. It is expected that more inhibitor molecules are adsorbed on the metal surface, increasing surface coverage at higher concentration of C8Na in the solution. Thus, the AA5052 surface is more efficiently separated from the aggressive medium at a high concentration of C8Na. This is indicated in Figure 3, showing that the increase in corrosion protection of aluminium observed by increasing C8Na concentrations up to a critical concentration of 0.01 M. However, addition 0.02 M C8Na to NaCl solution reduces the corrosion-inhibiting performance. This situation can be explained by the formation of aggregated micelles in solution when the concentration of C8Na is above a critical micelle concentration [22,23]. The corrosion-inhibiting tendency of C8Na still persists when

AA5052 is sliding contact with alumina under a load of 2N. However, the higher current density is recorded under abrasion condition, which results in lower IE%. The observations are obviously due to the destruction of the surface passive film and activation of the material inside the wear track. Therefore, anodic dissolution is accelerated by the rubbing action.

The adsorption of C8Na on the AA5052 surface not only provides corrosion-inhibiting performance but also changes the corrosive wear behaviour of AA5052 in 0.5M NaCl solution. Figure 9 shows the average COF and wear volumes for aluminium in NaCl solution in the absence and presence of C8Na. It is easy to observe that the addition of C8Na decreases the friction and wear of aluminium. Moreover, the tribological performance is potential-dependent. At the cathodic potential of -1.4 V vs Ag/AgCl, addition of C8Na to NaCl solution shows minor effect on the tribological performance of aluminium. Similar evolution of friction coefficient with sliding time and wear volume are observed for NaCl solution in the absence and presence of C8Na. In this case, the aluminium electrode is negatively charged, and the octanoate species are repelled from the aluminium surface through electrostatic effects. Thus, the adsorption of octanoate anions does not occur to any significant extent and wear of AA5052 at the cathodic potential of -1.4 V is mostly

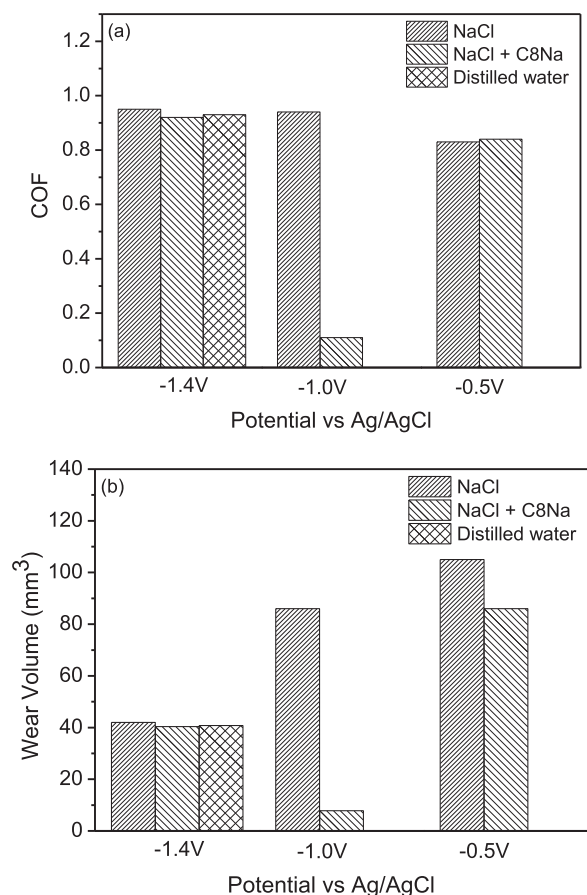


Figure 9. The variation of COF and wear volume at different potential applied for NaCl solution in the absence and presence of 0.01 M C8Na.

from pure mechanical. The effect can be also confirmed by conducting the tribocorrosion experiment at the same load in the presence of distilled water under nitrogen without applying potential. As shown in Figure 6, the friction curve recorded in distilled water coincides with that recorded at the potential of -1.4 V in the 0.5 M NaCl solution with and without 0.01 M C8Na. Moreover, three solutions show similar wear volumes (see Figure 9(b)). Thus, it may suggest that wear of AA5052 in our investigation is mostly from pure mechanical at the cathodic potential of -1.4 V.

At the anodic potential of -1.0 V vs Ag/AgCl, as shown in Figure 9, the wear volume of AA5052 specimen in the blank NaCl solution is found to be larger than at the cathodic potential of -1.4 V. The extra material loss can be explained from synergy between wear and corrosion [7–14]. Such a synergy effort for increasing wear volume is greatly hindered after addition of 0.01 M C8Na to the NaCl solution. Correspondingly, lower COF is observed for NaCl in the presence of C8Na than its absence. In this time, the aluminium electrode is oxidized and positively charged, helping to attract octanoate species to the electrode surface to form a film of aluminium octanoate. The film formed on the aluminium surface is effective in inhibiting corrosion and further reducing friction and

wear. In fact, alkanolic acid is generally considered as a friction modifier in the industry and has a promising effect on forming a brush-like structure on the surface thus reducing friction and wear in boundary conditions [24–26]. The similar results are observed before when alkanolic acid is used as a lubricating additive in water containing electrolyte [27–29].

When the potential is further increased to above -0.6 V vs Ag/AgCl, the pitting corrosion can be clearly observed on the wear track in the blank NaCl solution (Figure 8(b)). In this case, the total wear volume is largest, which is nearly three times magnitude larger than that at the cathodic potential of -1.4 V. The formation of pits inside the wear track has significant effects on friction and wear of AA5052. The pits on the wear track would reduce the real contact area inside the wear track, leading to higher contact stresses for subsequent contact cycles and then higher wear rates. Moreover, each pit can serve as a site for crack nucleation and a site of stress concentration, promoting crack initiation and propagation. Thus, the larger total wear volume is expected when the wear track is full of the more pits [12]. It is clearly observed that the addition of 0.01 M C8Na to NaCl solution is effective in protecting the surface from sever wear at the potential of -0.6 V vs Ag/AgCl. There is less pit found in the wear track (Figure 8(c)). Thus, the contribution of corrosion induced wear is expected to be lower in presence of C8Na, as indicated by a lower Faradaic reaction current measured during the experiment at the same potential.

The corrosive wear protection effect by addition C8Na in NaCl solution might have a practical application since it allows us to consciously control the formation of the protective aluminium carboxylate film to decrease friction of aluminium alloy even in aggressive NaCl solution.

5. Conclusion

- (1) The results here clearly show that C8Na molecules are effective in inhibiting the corrosion of aluminium in 0.5 M NaCl solution under both static immersion and abrasion conditions. The increase in corrosion protection of aluminium is observed by increasing C8Na concentrations up to a critical concentration of 0.01 M in NaCl solution.
- (2) The corrosive wear protection of C8Na in NaCl solution is potential-dependent. The addition of C8Na to NaCl solution shows minor effect on the tribological performance of aluminium at the cathodic potential of -1.4 V vs Ag/AgCl. The synergy effort between wear and corrosion for increasing wear volume is hindered at the anodic potential of -1.0 V and -0.6 V vs Ag/AgCl.
- (3) The tribocorrosion inhibition mechanism of AA5052 by octanoic anions is commonly

described by the hydrophobic character of the metal carboxylate film which is obtained by adsorption of carboxylate anions onto the aluminium surface. The inhibitive organic film is water repellent and forms a barrier for mass and charge transfer, which leads to a protection of the metal surface from the attack of chloride ions. The film also provides lower friction and better wear protection performance.

Acknowledgements

The authors thank Dr Shuyan Yang for her discussion.

Disclosure statement

No potential conflict of interest was reported by the authors.

Funding

This work was supported by National Natural Science Foundation of China [grant numbers 51375249, U1737214], Key Research & Development Plan of Shandong Province [grant number 2017GSF220012], Natural Science Foundation of Shandong Province [grant number ZR2017PEE013] and General Administration of Quality Supervision, Inspection and Quarantine of China [grant number 201410083].

References

- [1] Dursun T, Soutis C. Recent developments in advanced aircraft aluminium alloys. *Mater Design*. 2014;56:862–871.
- [2] Miller WS, Zhuang L, Bottema J, et al. Recent development in aluminium alloys for the automotive industry. *Mater Sci Eng A*. 2000;280:37–49.
- [3] Ezuber H, El-Houd A, El-Shawesh F. A study on the corrosion behavior of aluminum alloys in seawater. *Mater Design*. 2008;29(4):801–805.
- [4] Smialowska ZS. Pitting corrosion of aluminum. *Corros Sci*. 1999;41:1743–1767.
- [5] Panagopoulos CN, Georgiou EP, Gavras AG. Corrosion and wear of 6082 aluminum alloy. *Tribol Int*. 2009;42:886–889.
- [6] Liu Y, Mol JMC, Janssen G. Combined corrosion and wear of aluminium alloy 7075-T6. *J Bio-Tribo-Corros*. 2016;2:9.
- [7] Pokhmurskii VI, Zin IM, Vynar VA, et al. Contradictory effect of chromate inhibitor on corrosive wear of aluminium alloy. *Corros. Sci*. 2011;53:904–908.
- [8] Mischler S. Triboelectrochemical techniques and interpretation methods in tribocorrosion: a comparative evaluation. *Tribol Int*. 2008;41(7):573–583.
- [9] Ponthiaux P, Wenger F, Drees D, et al. Electrochemical techniques for studying tribocorrosion processes. *Wear*. 2004;256(5):459–468.
- [10] Mischler S, Debaud S, Landolt D. Wear-accelerated corrosion of passive metals in tribocorrosion systems. *J Electrochem Soc*. 1998;145(3):750–758.
- [11] Cakmak E, Tekin KC, Malayoglu U. Tribocorrosion of Stellite 706 and Tribaloy 400 superalloys. *Tribol – Mater, Surf Interfaces*. 2010;4:8–14.
- [12] Sun Y, Rana V. Tribocorrosion behaviour of AISI 304 stainless steel in 0.5 M NaCl solution. *Mater Chem Phys*. 2011;129(1–2):138–147.
- [13] Zhang Y, Wang JZ, Yin XY, et al. Tribocorrosion behaviour of 304 stainless steel in different corrosive solutions. *Mater Corros*. 2016;67(7):769–777.
- [14] Bidiville A, Favero M, Stadelmann P, et al. Effect of surface chemistry on the mechanical response of metals in sliding tribocorrosion systems. *Wear*. 2007;263(1–6):207–217.
- [15] Garcia I, Drees D, Celis JP. Corrosion-wear of passivating materials in sliding contacts based on a concept of active wear track area. *Wear*. 2001;249(5–6):452–460.
- [16] Aballe A, Bethencourt M, Botana FJ, et al. CeCl₃ and LaCl₃ binary solutions as environment-friendly corrosion inhibitions of AA5083 Al-Mg alloy in NaCl solutions. *J Alloys Compd*. 2001;323–324:855–858.
- [17] Yasakau KA, Zheludkevich ML, Sviatlana V, et al. Mechanism of corrosion inhibition of AA2024 by rare-earth compounds. *J Phys Chem B*. 2006;110:5515–5528.
- [18] Sherif EM, Park SM. Effects of 1, 4-naphthoquinone on aluminum corrosion in 0.50 M sodium chloride solutions. *Electrochimica Acta*. 2006;51:1313–1321.
- [19] Boisier G, Portail N, Pébère N. Corrosion inhibition of 2024 aluminium alloy by sodium decanoate. *Electrochimica Acta*. 2010;55:6182–6189.
- [20] Daloz D, Rapin C, Steinmetz P, et al. Corrosion inhibition of rapidly solidified Mg-3% Zn-15% Al magnesium alloy with sodium carboxylates. *Corrosion*. 1998;54:444.
- [21] Zucchi F, Grassi V, Zanotto F. Sodium monocarboxylates as inhibitors of AZ31 alloy corrosion in a synthetic cooling water. *Mater Corros*. 2009;60:199–205.
- [22] Rocca E, Bertrand G, Rapin C, et al. Inhibition of copper aqueous corrosion by non-toxic linear sodium heptanoate: mechanism and ECAFm study. *J Electroanal Chem*. 2001;503(1–2):133–140.
- [23] Zhao T, Mu G. The adsorption and corrosion inhibition of anion surfactants on aluminium surface in hydrochloric acid. *Corros Sci*. 1999;41:1937–1944.
- [24] Zhang Q, Wan Y, Li Y, et al. Friction reducing behaviour of stearic acid on a textured aluminium substrate. *Appl Surf Sci*. 2013;280:545–549.
- [25] Loehlé S, Matta C, Minfray C, et al. Mixed lubrication of steel by C18 fatty acids revisited. Part I: toward the formation of carboxylate. *Tribol Int*. 2015;82:218–227.
- [26] Sahoo RR, Biswas SK. Frictional response of fatty acids on steel. *J Colloid Interface Sci*. 2009;333:707–718.
- [27] Zhu YY, Kelsall GH, Spikes HA. The influence of electrochemical potentials on the friction and wear of iron and iron oxides in aqueous systems. *Tribol Trans*. 1994;37(4):811–819.
- [28] Brandon NP, Bonanos N, Fogarty PO, et al. The effect of interracial potential on friction in a model aqueous lubricant. *J Electrochem Soc*. 1992;139(12):3489–3492.
- [29] Meng Y, Jiang H, Wong PL. An experimental study on voltage-controlled friction of alumina/brass couples in zinc stearate/water suspension. *Tribol Trans*. 2001;44(4):567–574.